Performance of a Solar-Powered Robot for Polar Instrument Networks

J.H. Lever
Cold Regions Research and Engineering Laboratory
US Army Engineer Research and Development Center
Hanover, NH 03755
james.h.lever@erdc.usace.army.mil

A. Streeter and L.R. Ray
Thayer School of Engineering
Dartmouth College
Hanover, NH 03755
Laura.E.Ray@Dartmouth.EDU

Abstract **– The *Cool Robot* is a four-wheel-drive, solar-powered autonomous vehicle designed to support summertime science campaigns in Antarctica and Greenland. We deployed the robot at Summit Camp, Greenland, during 2005 to validate its power budget and to assess its unique control system that matches solar power input with power demand as the robot drives over rough terrain. The 61-kg robot drove continuously at 0.78 m/s on soft snow, its 160-W average power demand met by solar power alone under clear skies when sun elevation exceeded 16°. The power-control system reliably matched input with demand as insolation changed during the tests. A simple GPS waypoint-following algorithm provided reliable autonomous navigation over periods of 5 - 8 hours. The data validate our design models and indicate that the *Cool Robot* will exceed its design goal of carrying a 15-kg payload 500 km in two weeks on the Antarctic plateau.**

Index Terms **- mobile robot design, power system control.**

I. Introduction

About 70 – 85% of the budget for the U.S. Antarctic and Arctic research programs pays for logistics. Autonomous mobile robots could significantly reduce this logistics burden and thus expand the scientific utilization of Antarctica and Greenland by creating networks of instruments that can be tailored to specific experiment plans. Campaigns include snow characterization and biological sampling along transects and upper atmosphere or magnetosphere observations using broadly spaced instrument arrays.

Antarctica poses numerous challenges for mobile robots, including extreme low temperatures, blowing snow and vast distances. Nevertheless, it is possible to capitalize on conditions unique to polar snowfields to design a simple robot capable of long-distance autonomous travel. During Antarctic summers, the sun is above the horizon all day and the skies are frequently clear. Thus, solar power is attractive assuming summertime deployments are acceptable. Firm snow permits use of low-pressure wheels, which are preferred over tracks for simplicity and mechanical efficiency. Four-wheel-drive (4WD) provides good mobility and is consistent with high reliability and low cost. Vast tracts of the Antarctic plateau and neighbouring ice shelves are obstacle free provided the vehicle can negotiate wind-sculpted sastrugi that are commonly 0.3-m high at 2-m wavelengths.

Based on this reasoning, we designed the 4WD solar-powered robot *Cool Robot* (Fig. 1) to deploy summertime instrument networks in Antarctic [1]. Its goal is to carry a 15-kg payload a distance of 500 km in two weeks using GPS waypoint navigation. A lightweight honeycomb chassis holds the electronics, batteries, and four brushless DC motors, each directly driving a low-pressure tire. A five-sided box of solar panels surrounds the chassis, collecting solar power reflected from the snowfield as well as directly incident to the panels. A unique power-management system controls the operating point of each panel to match collective power input to power demand, even as insolation changes while the robot moves over rough terrain. The robot measures 1.2 x 1.2 x 1.0 m.

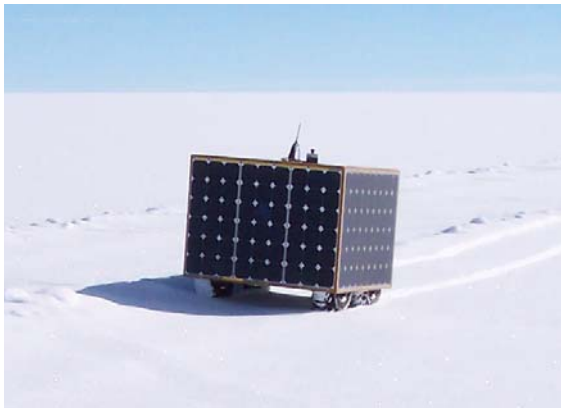

Fig. 1 *Cool Robot* driving autonomously under solar power in Greenland.

We recently deployed the *Cool Robot* at Summit Camp, Greenland, to assess its design. This paper briefly describes the robot's mobility and power systems and presents data from Greenland that validate the key features of its design.

II. Mobility Design

Rolling resistance predominates the power budget of over-snow vehicles. Also, peak traction on snow determines whether the vehicle can develop sufficient thrust to overcome resistance, climb a slope or pull a load. Thus careful design for over-snow mobility is required for polar robots. The semi-empirical theory of Bekker [2, 3] offers simple approaches to estimate vehicle resistance and traction on snow.

Rolling resistance, R, of a wheeled vehicle on level, deformable terrain is the sum resistance from tire deformation, R_t, and compaction of the terrain, R_c. Tire-deformation resistance is usually expressed as a dimensionless coefficient, R_t/W, where W is the vertical force on the tire. It is difficult to

predict but generally increases with decreasing inflation pressure. Based on tests of similar tires, $R_t/W = 0.09$ is a conservative estimate for the *Cool Robot* tires.

Bekker theory relates the work to compact deformable terrain derives to its pressure-sinkage relationship:

$$p(z) = kz^n \quad (1)$$

where p is pressure, z is sinkage, and k and n are parameters characterizing the terrain. When the tire is soft relative to the snow, a flat-bottomed contact patch supports most of the vertical force. For this case

$$R_c = bk(z_0)^{n+1}/(n+1) \quad (2)$$

where b is tire width and z_0 is found by inverting (1) for tire contact pressure p_0.

Snow packs tend to respond linearly to small indentation ($n = 1$). Values of k are difficult to obtain, but traveling over hundreds of kilometers of Antarctica provided the following observations: (a) hard snow surfaces such as sastrugi do not deform under boot pressures (25 – 50 kPa); (b) typical sinkage under boot pressure is 2 – 5 cm and rarely exceeds 10 cm, suggesting k ~ 1 MPa is conservative for Antarctic snow.

The *Cool Robot* tires measure 0.51-m-dia. x 0.15-m-wide. They support the vehicle at zero inflation pressure owing to carcass stiffness. Measured contact patches indicate that, at the design weight of 200 N per wheel and zero inflation, $p_0 =$ 20 kPa. Using these values, (1) and (2) predict $z_0 \sim 2.0$ cm and $R_c/W \sim 0.15$ for Antarctic snow. Adding tire-deformation resistance, $R/W = 0.24$ should be conservative for total rolling resistance of the *Cool Robot* on Antarctic snow.

A vehicle can move over snow if it develops traction in excess of motion resistance. A dimensionless equation for net traction, T_n, is

$$T_n/W = T_g/W - (R_t/W + R_c/W) \quad (3)$$

where T_g is the gross traction developed by the wheels. This equation applies for horizontal, straight-line travel and defines the reserve for towing a trailer, climbing a slope or accelerating. When $T_n < 0$, the vehicle is immobilized. Also, to make headway the motor must supply a drive force equal to the sum of gross traction and internal friction.

Shear failure in the snow under the contact patch limits gross traction. Bekker theory assumes that the maximum shear stress, τ, is governed by a Mohr-Coulomb criterion:

$$\tau = c + p \tan\Phi \quad (4)$$

where c is the cohesion and Φ is the internal angle of friction within the snow. For small sinkage and uniform contact pressure, (4) converts to an equation for gross traction:

$$T_g/W = c/p_0 + \tan\Phi \quad (5)$$

Thus, lightweight vehicles with p_0 can achieve high T_g/W owing to the increased importance of snow cohesion.

Measurements of c and Φ for snow vary broadly, with most values ranging $c \sim 1 – 10$ kPa and $\Phi \sim 15 – 25°$ [3 - 5]. Unfortunately, no data are available for Antarctic snow. Traction tests conducted on the McMurdo Ice Shelf indicate $T_g/W \sim 0.46$ for tractors with average ground pressure of 50 kPa [6]. Because the snow was well bonded, cohesion was probably high, say $c \sim 10$ kPa, and (5) would suggest $\Phi \sim 15°$ for that snow. Consequently, $T_g/W \sim 0.8$ for the *Cool Robot* at $p_0 = 20$ kPa in similar snow. Allowing for rolling resistance via (3), the *Cool Robot* should be able to develop net traction $T_n/W \sim 0.5$, sufficient to climb a 30-degree slope or tow a substantial load behind it.

III. Power Budget

Solar power reflected from a snowfield supplements the direct-incidence power striking a photovoltaic panel [7]. For solar irradiance p_s (W/m^2) striking a snowfield at elevation angle ϕ, the irradiance reflected to a vertical panel is

$$p_r = \alpha\, IF\, p_s \sin\phi \quad (6)$$

where α is the snow albedo and IF is an integral factor that accounts for the distance away from the panel at which the snow ceases to appear as a perfectly diffuse reflector. Note that (6) applies even when the panel faces away from the sun and receives no direct irradiance.

Measurements made on the Ross Ice Shelf, Antarctica, using a precision spectral pyranometer (PSP) under clear skies provide values for the product αIF for vertical panels in orthogonal directions: 0.40 facing sun, 0.54 edge-on to sun, and 0.41 facing away from sun [7]. Also, p_s averages 1,000 W/m^2 at South Pole during the four months of the summer season, confirming that clear skies predominate on the polar plateau [8]. Using these values and estimates for conversion efficiencies of the solar panels (0.18) and power conditioning circuits (0.95), a *Cool Robot* consisting of five 54-cell solar panels should produce about 240 W of electrical power when the sun is only 15° above the horizon. Note that 30% of this power derives from sunlight reflected from the snowfield. For $R/W = 0.24$, motor-gearbox efficiencies of 0.72 and housekeeping power of 25 W, a total power of 240 W would allow the 80-kg robot with payload to drive continuously at 0.8 m/s, or twice the average speed needed to meet its goal of traveling 500 km in two weeks.

Similar analyses show that for sun elevations exceeding 24°, the robot can drive at its maximum speed of 1 m/s with a power surplus. Conversely, the robot will need to drive at reduced speed under cloudy or low sun elevation conditions. A major role of the power control system is thus to match power input to power demand.

IV. Control of Photovoltaic Power System

Fig. 2 shows the *Cool Robot* power system. It is operated by a microcontroller that is slaved to a master microcontroller; the latter generates motor commands for navigation. Three lithium-ion batteries establish ~ 48-V bus, onto which each solar panel delivers power through its own DC/DC converter. Additional converters provide housekeeping power for electronics, microcontrollers, and payload. The power system implements various control modes to meet mobility and housekeeping power demand.

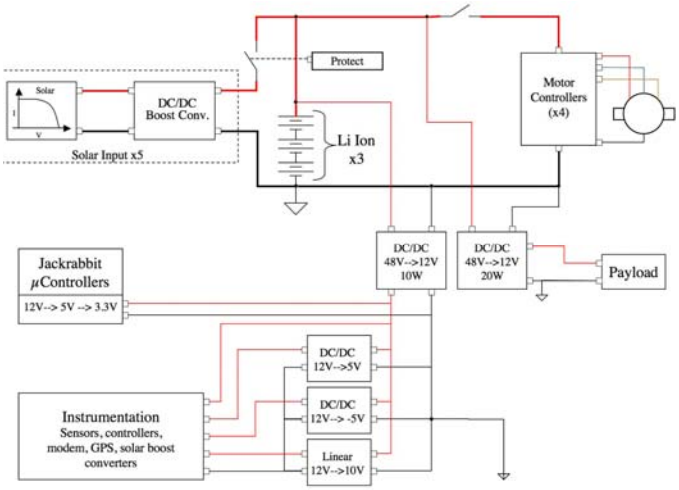

Fig. 2 *Cool Robot* power system.

The core focus of the system is to control the DC/DC converters for each solar panel. In most photovoltaic systems, a control algorithm operates a panel at its Maximum Power Point (MPP) – the current-voltage (I-V) setpoint that maximizes power output. Fig. 3 shows how typical panel I-V characteristics vary with temperature and insolation. For the *Cool Robot*, insolation can change on each panel at relatively high bandwidth (0.5 to 1 Hz) as the robot traverses rough terrain. Load will also vary under these conditions. Thus, the power-point tracking control algorithm must exhibit robust tracking performance in the face of these variations.

In the *Cool Robot*, the large-signal input impedance of each panel's DC/DC converter can be adjusted by modulating the converter's duty cycle, *D*. Relative to the modulation frequency, the load is approximately a fixed resistance *R,* and the output voltage, V_{out} , is the nearly constant bus voltage. Thus, for an ideal boost converter,

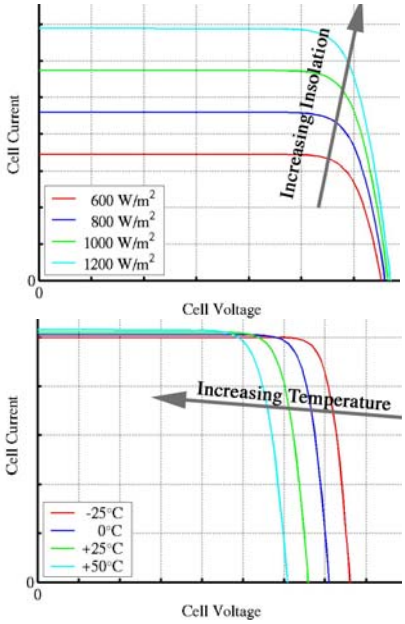

Fig. 3 Solar panel I-V characteristics.

$$V_{in} I_{in} = V_{out} I_{out} = \frac{V_{out}^2}{R} = \frac{1}{R}\left(\frac{V_{in}}{1-D}\right)^2 \qquad (7)$$

and the large-signal input impedance of the converter, $R(1-D)^2$, appears to the solar panel as a load that varies with duty cycle. Thus, by varying duty cycle, one can traverse the I-V curve of the panel to operate at maximum power or at a setpoint that matches power demand. To do this in real-time, the operating point must be constantly monitored and duty cycle updated to reflect any changes.

The bandwidth of insolation and load variation led to development of a non-model-based "perturb and observe" (PAO) nonlinear MPPT algorithm. It does not require *a priori* knowledge of the electrical characteristics of the panel being controlled. The algorithm drives the derivative of panel power *P* with respect to duty cycle towards zero. However, to measure $\partial P/\partial D$, a change in *P* is necessary, either explicitly through the control command, or implicitly from the natural operation of the system. While PAO methods are straightforward to implement, they operate *around* the MPP rather than on it, due to this perturbation.

Sullivan and Powers [9] present an MPPT for a solar racing vehicle. As in the *Cool Robot*, the output of the power electronics is a connected to a battery-clamped bus. Therefore, one need measure only the output current to determine the power setpoint. The output current of the MPPT is monitored because the control goal is to maximize the power delivered to the system, which may not correspond exactly to the MPP of the panel. Thus, the overall control goal is to force $\partial I_{out}/\partial D = 0$. The perturbation on *D* is produced through a "clocked auto-oscillation method," causing the controller to climb steadily up the power curve from either side, until it reaches and passes the MPP and the sign of $\partial I_{out}/\partial D$ changes, forcing the controller to switch direction and head back to the MPP. This "bang-bang" control benefits from not requiring a detailed model of the solar panel or electronics characteristics.

Following [10], the *Cool Robot* MPPT algorithm is implemented using a microcontroller with $\partial P/\partial D$ estimated as the discrete change $\Delta P/\Delta D$ between two time steps. It runs at a sampling rate of 10 - 40 Hz, and has an adaptive step size

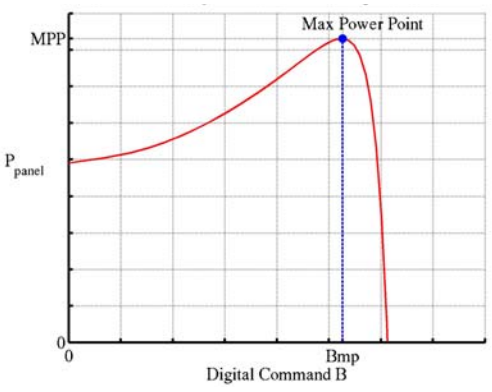

Fig. 4 Relationship between digital command *B* and panel power.

proportional to $\Delta P/\Delta D$. In this way, when the algorithm is far from the MPP, it uses a large change in duty cycle to more rapidly reach it. As the algorithm converges to the MPP, the step size decreases.

The duty cycle is not explicitly commanded. Rather, the power microcontroller sends a 12-bit number, *B*, to the digital to analog converter, which provides a 0-5 V analog command to the DC/DC boost converter to set *D*. The relationship between *B* and *D*, found experimentally, can be represented by a trigonometric function. Fig. 4 shows the resulting *P-B* relationship for a panel. The gently curving area to the left of the MPP represents the constant current portion of the I-V curve, while the steeper portion to the right of the MPP is the constant voltage portion.

In Fig. 4, the MPPT algorithm would increase *B* when $\partial P/\partial B$ is positive, and decrease *B* when $\partial P/\partial B$ is negative. However, shifts in the *P-B* curve due to changes in insolation make this task more difficult. For a slowly varying *P-B* curve, tracking the MPP is relatively easy. However, when the robot traverses uneven terrain, changes in orientation of the five solar panels with respect to the sun can cause insolation on each panel to vary substantially, changing the shape and amplitude of the *P-B* curve. For sastrugi with wavelengths of 1-2 meters traversed at the robot's maximum speed, the frequency will be 0.5 – 1 Hz. The resulting changes in a panel's I-V characteristics are much faster than those resulting from the sun's motion or changes in panel temperature. This is a unique control challenge for the *Cool Robot* compared to stationary photovoltaic installations. Depending on the speed of the algorithm, such rapid changes could cause poor tracking of the MPP, or worse, unstable performance.

If the controller operates much faster than changes in the *P-B* curve, however, the system can operate correctly. This is shown in Fig. 5, where a decrease in insolation has shifted the *P-B* curve downward. Based on conditions at time t_k, the algorithm commands a decrease in *B* to move towards the MPP. Provided the curve shift is small before the next controller time step t_{k+1}, the duty cycle change ΔB_{k+1} will produce a correct, if slightly reduced, movement of the operating point up the power curve. The calculated slope, $\Delta P'_{k+1}/\Delta B_{k+1}$, is smaller than expected but will have the correct sign, so that the controller will move on correctly to time step t_{k+2}.

In this example, it is assumed that the controller operates the solar panel to the right the MPP on the *P-B* curve, where

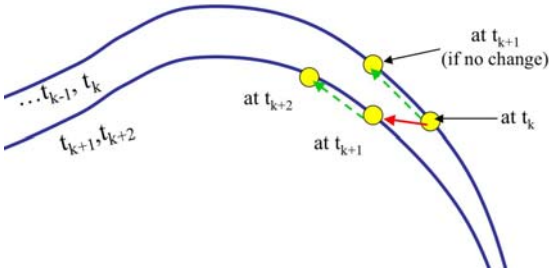

Fig. 5 MPPT algorithm operation when its sample rate is fast compared to the rate of change in the P-B curve.

panel voltage is approximately constant and the current changes greatly. This decision is intentional as the boost converter operates more efficiently when the voltage ratio between input and output is near unity. Also, susceptibility of the MPPT algorithm to changes in insolation and measurement noise is less when the slope of the *P-B* curve is steep. As the tracking algorithm oscillates about the MPP, the operating point will inevitably spend some time to the left of the MPP. However, the algorithm can detect this because $\Delta P/\Delta B$ is then positive. It will then increase *B* to traverse back to the right side of MPP. Simulation of the control algorithm's response to 0.5 – 1 Hz curve shifts and noise in the power measurements showed robust performance and tracking efficiencies exceeding 90% provided sampling frequencies exceeded about 40 Hz [11]. Here we define tracking efficiency as the instantaneous ratio between the power at the panel's operating point and the true maximum power point.

The normal power-system control goal is to match power demand when possible, and when not possible, request a speed reduction to reduce demand. Available power that is not extracted from a panel is dissipated as heat through its surface. Were MPPT used continually on all panels, the excess power would have to be disposed of, for example through a resistor bank, at added weight and complexity. The approach used here is to minimize the average current flowing into or out of the batteries. When the power delivered by the panels exactly matches that needed by the robot, the batteries will not be utilized and the current through them will be zero. Specifically, the control goal under normal conditions is to minimize battery current by adjusting duty cycle commands to the five DC/DC boost converters. Operation under special conditions (e.g., to charge the batteries, to operate a payload when stationary, etc.) are straightforward to implement.

For the batteries to be effective buffers for the power bus, they need to accept power as well as provide it. The setpoint chosen for the control algorithm is a battery stack voltage of 48.6 V, or roughly 80% state-of-charge, which allows the batteries to accept or deliver 3 A of current instantaneously to smooth power fluctuations.

The power system uses a nested bang-bang control law. The inner loop consists of five independent loops, one for each DC/DC boost converter. The outer loop monitors the battery current and calls for more or less power from the inner loops accordingly. When the outer loop calls for more power, the control effort for each DC/DC converter is to seek more power through maximum power-point tracking; when the outer loop calls for less power, the control effort is to migrate each solar panel away from its MPP and towards the open-circuit voltage of each panel (the right side of Fig. 4). The DC/DC converter for each panel can also be disabled until there is a greater demand for power. At the opposite end of the spectrum, when all of the panels are operating near their respective MPPs and the power produced is insufficient to meet demand, the power microcontroller will inform the master microcontroller that the robot must slow down.

V. Greenland Experiments

Summit Camp, operated by the National Science Foundation, is located in central Greenland at 38.46° W, 72.58° N and altitude 3,200 m. Away from the buildings and 4-km-long skiway, the level, undisturbed snow surface in late July through early August, 2005, was much softer than typical Antarctic snow, and sinkage ranged 10 – 30 cm under boot pressure. The groomed skiway did not yield under boot pressure but was at times covered with 2 – 5 cm of fresh, light snow. In effect, the natural and skiway surfaces bracketed snow hardness typical of Antarctic terrain. All snow surfaces were brilliant white, and air temperatures ranged from about -5 at noon to -20 C around midnight.

The *Cool Robot* test mass was 61 kg, including a 1-kg datalogger. This compared favorably with the design empty mass of 65 kg and produced tire contact pressures of 15 kPa with the tires deflated. The datalogger recorded the current and speed of each motor at 1 Hz and logged 10-s average values. The motor-gearbox torque constant (8.55 Nm/A) and tire rolling radius (0.228 m) convert measured motor currents and speeds to gross traction and vehicle speed (the latter for negligible slip). The datalogger similarly recorded vehicle sinkage, based on distance to the snow surface measured by an ultrasonic sensor, and stored current, voltage and duty cycle values provided by the power microcontroller for each solar panel. Other instrumentation included a load cell to measure drawbar pull, a device to measure the snow pressure-sinkage relationship, a snow-density kit, and a PSP to measure direct and reflected solar irradiance.

Initial tests, conducted on battery power, confirmed that the *Cool Robot* could drive over the soft, undisturbed snow surface. Traction tests involved towing a small sled loaded with 1 – 3 persons and measuring the towing forces (Fig. 6). Tests to validate the solar power system progressed from one to four panels as we systematically resolved issues with the control hardware and algorithm. Unfortunately, we resolved a particularly resilient initialization error only after losing one DC/DC converter and all spare parts, so that the *Cool Robot* operated on only four of five solar panels for the long-duration tests. Autonomous navigation was accomplished using a simple GPS waypoint-following algorithm with open-loop motor-speed corrections in response to angular deviations from the desired waypoint [12].

VI. Results

Rolling resistance data were available from most tests. During the five-hour test conducted on 7 Aug 05, resistance on undisturbed snow averaged $R/W = 0.21 \pm 0.03$ while sinkage averaged $z = 5.6 \pm 0.8$ cm ($\pm$ 1 σ). Shorter tests conducted on the skiway produced average R/W ranging 0.09 – 0.11 with sinkage averaging less than 1 cm. These results should bracket the resistance and sinkage on typical Antarctic snow and suggest that the design estimates are conservative.

Fig. 6 *Cool Robot* pulling a sled on the skiway during traction tests.

Traction tests conducted on the skiway gave maximum values of $T_g/W = 0.46 \pm 0.05$ and $T_n/W = 0.30 \pm 0.05$ when the *Cool Robot* towed three persons in the sled. These values are less than design estimates, but because the robot did not break traction, they likely underestimate peak values possible on firm Antarctic snow. Indeed, the robot towed continuously a mass exceeding 3.5 times its own mass, indicating that it should easily be able to tow a significant science payload in Antarctica. Obstacle-crossing tests showed that the *Cool Robot* could easily climb 0.3-m-high, steep-faced berms (Fig. 7).

A long-duration test conducted on 7 Aug 05 produced several important results. Skies were mostly clear, but faint

Fig. 7 *Cool Robot* 0.3-m high snow berm.

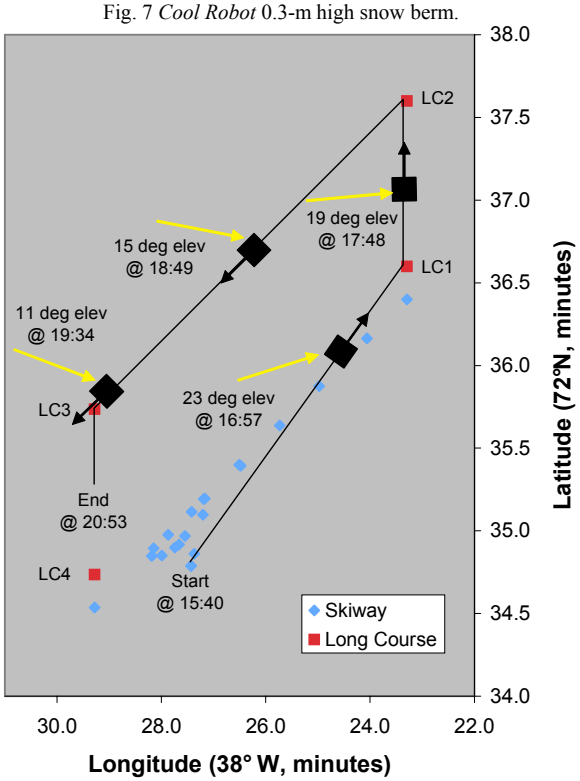

Fig. 8 *Cool Robot* path during long-duration test on 7 Aug 05. Black boxes and arrows indicate Cool Robot location and direction of travel at the time and sun elevation indicated. Yellow arrows indicate the corresponding direction of the direct solar irradiance.

clouds ringed the horizon and decreased solar irradiance as the sun set. With four solar panels operating, the *Cool Robot* drove autonomously for five hours, navigating a course of four waypoints laid out on level, undisturbed snow north of the skiway (Fig. 8). Fig. 9 shows a timeseries plot of the power budget. After it crossed the skiway (16:42), the robot's average power demand was 160 W. The control system successfully operated the solar panels to meet power demand until 18:33, at which time sun elevation was 15.9° and the sun was partly obscured by faint clouds. Prior to this, average battery power was zero, although both battery and solar panel power fluctuated ± 40 W in response to variations in motor power and controller performance. After it could not meet the power demand, the control system operated the four panels at their respective MPPs and the rapid fluctuations in panel output power essentially disappeared. Battery power output increased to make up the shortfall. When the skies cleared briefly at 19:20, the panels provided all but 7 W of the power demand. These results are consistent with those predicted by the model used to estimate the robot's power budget.

Average speed was 0.78 m/s while the panels were able to meet the power demand. Later, as battery power increased, bus voltage and consequently vehicle speed decreased. The robot stopped at 20:53 when the bus voltage dropped below 43 V. For this test, the control system did not include a link allowing the power microcontroller to request that the master controller slow down the robot to reduce power demand.

A repeat of this test on 8 Aug 05 lasted 8 hours and produced similar results. For this second long-duration test, the master microcontroller twice executed controlled, 1-hr shut downs to recharge the batteries when their voltage dropped below 43 V. A minor error in the navigation algorithm ended the test as the robot attempted to conduct a second loop around the test course.

VII. Conclusions

The *Cool Robot* successfully demonstrated good mobility at Summit Camp over snow that was much softer than typical terrain in Antarctica. Its rolling resistance was lower than design estimates, suggesting that power demand on firm Antarctic snow will be less than predicted. Traction tests, both quantitative and qualitative, provide confidence that the *Cool Robot* will be able to tow significant science payloads and negotiate commonly occurring Antarctic sastrugi.

Particularly encouraging was the reliable performance of the power control system. With sufficient solar input, it operated the four solar panels to match their power output with power demand. As solar input decreased below the match point, it operated all panels at their maximum power points. Although the snow surface was smooth, the algorithm performed well as the robot executed numerous turns and steering corrections during which solar insolation varied rapidly. It should thus be able to match power demand on rough Antarctic terrain that produces similarly rapid isolation changes. Lastly, the autonomous navigation algorithm performed reliably during two test lasting 5 – 8 hours.

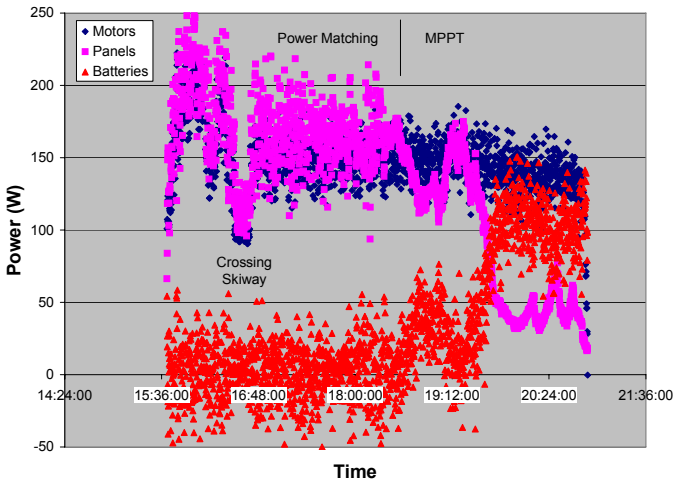

Fig. 9 Power budget during 7 Aug 05 long-duration test.

Collectively, these results validate the basic design of the 4WD, solar-power *Cool Robot*. It should exceed its goal carrying a 15-kg payload across 500 km of the Antarctic plateau in less than 2 weeks.

Aknowledgements

This work is supported by NSF grant OPP-0343328, NIST grant 60NANB4D1144, Army AT42 work unit Mobility of Lightweight Robotic Vehicles, and grant 2005-DD-BX-1091 awarded to the Institute for Security Technology Studies by the Bureau of Justice Assistance.

References

[1] L. Ray, A. Price, A. Streeter, D. Denton and J.H. Lever, "Design of a mobile robot for instrument network deployment in Antarctica," Proceedings of the 2005 IEEE International Conference on Robotics and Automation, Barcelona, Spain, April 2005, pp. 2123 – 2128.

[2] M.G. Bekker, *Theory of Land Locomotion*. University of Michigan Press, Ann Arbor, MI, 1956.

[3] J.Y. Wong, *Theory of Ground Vehicles* (2nd ed). Wiley-Interscience, Wiley & Sons, New York, 1993.

[4] M. Mellor, *Oversnow Transport*. Cold Regions Science and Engineering Monograph III-A4, Cold Regions Research and Engineering Laboratory, Hanover, NH, 1963.

[5] T. Muro and J. O'Brien, *Terramechanics*. A.A. Balkema Publishers, Lisse, Netherlands, 2004.

[6] J.H. Lever, J.C. Weale, R.G. Alger, and G.L. Blaisdell, *Mobility of Cargo Trains during Year Two of the Proof-of-Concept South Pole Traverse*. ERDC/CRREL Technical Report TR-04-22, Cold Regions Research and Engineering Laboratory, Hanover, NH, 2004.

[7] J.H. Lever, L.R. Ray, A. Streeter and A. Price, Solar power for an Antarctic rover, *Hydrological Processes,* 2006 (in press).

[8] Climate Monitoring and Diagnostic Laboratory (CMDL), http://www.cmdl.noaa.gov/info/ftpdata.html, accessed March 2004.

[9] C. Sullivan and M. Powers, A high efficiency maximum power point tracker for photovoltaic arrays in a solar-powered racing vehicle. *Proceedings of the 24th IEEE Power Electronics Specialists Conference*, June 1993, pp. 574-580.

[10] P. Bhide and S.R. Bhat, Modular power conditioning unit for photovoltaic applications." *Proceedings of the 23rd IEEE Power Electronics Specialists Conference*, June – July 1992, vol 1, pp. 708-713.

[11] G. Dietrich and T. Zettl, *Communication, Navigation and Control of an Autonomous Mobile Robot for Arctic and Antarctic Science*, B. Eng. Thesis, Thayer School of Engineering, Dartmouth College, April 2005.